

1 **Water availability dynamics have long-term effects on mature**
2 **stem structure in *Vitis vinifera***

3 S. Munitz^{1,2*}, Y. Netzer^{1,2*}, Ilana Shtein^{1,2} and A. Schwartz¹

4 ¹ R.H. Smith Institute of Plant Science and Genetics in Agriculture, Faculty of Agriculture, Food
5 and Environment, The Hebrew University of Jerusalem, Rehovot 76100, Israel.

6 ² The Eastern Regional Research and Development Center, Ariel 40700, Israel.

7

8 E-mail addresses:

9 sarel.munitz@mail.huji.ac.il ilanash@ariel.ac.il ammon.schwartz@mail.huji.ac.il

10 Corresponding author:

11 Y. Netzer, y-netzer@gmail.com, +972546320280

12 Number of tables: 2, number of figures: 7, word count: 4543 , date of submission: 11/02/18

13

14 **Running title:** Anatomical structure is affected by early season water availability.

15

16 **Highlights:**

17 Water availability early in the season determines vegetative growth and stem anatomical structure
18 in mature *Vitis vinifera* vines.

19

20 **Abstract:**

21 *Vitis vinifera* is a climbing vine with wide vessels and high hydraulic conductivity. There is a
22 lack of data on the anatomical structure of the mature vine stem, and most current knowledge is
23 based on first-year shoots. Moreover, the effect of drought stress on anatomical structure has
24 been partly reported in shoots of *Vitis vinifera* but not in stems.

25 In current study two irrigation approaches were applied on *Vitis vinifera* Merlot vines: constant
26 (low, medium and high irrigation) and dynamic (early/late season water deficit). The following
27 parameters were measured: trunk diameter, annual ring width and area, vessel diameter, specific
28 hydraulic conductivity and stem water potential.

29 High water availability early in the season (high irrigation and late deficit) resulted in vigorous
30 vegetative growth (greater trunk diameter, ring width and area), wider vessels and increased

31 specific hydraulic conductivity. The distribution of large xylem vessels was altered by drought
32 stress, where high water availability early in the season caused a shift of the vessel population
33 towards the wider frequency classes. Interestingly, the early deficit vines showed more negative
34 water potential values late in the season compared to the low irrigation vines. This may imply an
35 effect of anatomical structure on vine water status.

36 **Key words:** Drought stress, specific hydraulic conductivity, vessel diameter, vessel distribution,
37 *Vitis vinifera*, water availability.

38 **Introduction**

39 The genus *Vitis* has been distinguished for its wide (Adkinson 1913; Pratt 1974)
40 and long xylem vessels (Zimmermann and Jeje 1981; Ewers et al. 1990;
41 Jacobsen et al. 2012), which characterize lianas. Such hydraulic architecture
42 makes *Vitis vinifera* an excellent model of water flow in plants according to the
43 "unit pipe model" as described by Tyree & Ewers (1991), since *Vitis* vessels are
44 relatively optimal pipes. Since vessel length and diameter are correlated with
45 stem diameter, mature vine trunks tend to have wider and longer vessels
46 compared to young stems/shoots (Ewers and Fisher 1989; Jacobsen et al. 2012;
47 Hacke 2015). Moreover, since vessels in *Vitis* are completely inactivated after 4
48 to 7 years (Tibbetts and Ewers 2000), in mature vine trunks (older than 7 years)
49 only the secondary xylem is functional, while the primary xylem created in its
50 first year is nonfunctional. This fact is crucial, since in contrast to the scalariform
51 arrangement of intervessel bordered pits of secondary xylem vessel elements, the
52 primary xylem vessel elements have partial secondary wall thickenings, making
53 them much more vulnerable to cavitation (Pratt 1974; Choat et al. 2005; Sun et
54 al. 2006; Brodersen et al. 2011; Craig R Brodersen et al. 2013; Rolland et al.
55 2015; Hochberg, Herrera, et al. 2016). Indeed, visualization techniques (microCT
56 / MRI) have shown that in one-year-old stems of *Vitis* the spread of embolism
57 proceeds from the pith towards the cambium through the primary xylem (Choat
58 et al. 2010; Craig R Brodersen et al. 2013; Craig Robert Brodersen et al. 2013;
59 Knipfer et al. 2015; Hochberg, Albuquerque, et al. 2016). An additional
60 important anatomical feature of mature vine trunks is the ratio between the area
61 of the pith and the xylem, which decreases with stem maturation (Sun et al.
62 2006). All of the above suggest that the xylem architecture of the mature trunk

63 differs from that of a young shoot, in a way that makes it less vulnerable to
64 cavitation.

65 Despite those significant differences, there is a scarcity of information about the
66 anatomical structure of mature vine trunks, while current reported anatomical
67 information on vines is based mainly on analysis of one-year-old stems (Schultz
68 and Matthews 1993; Lovisolo et al. 1998; Schubert et al. 1999; Sun et al. 2006;
69 Brodersen et al. 2011; Chatelet et al. 2011; Santarosa et al. 2016). In one-year-
70 old stems, hydraulic structure is reported to vary among *Vitis* cultivars and
71 rootstocks (Chouzouri and Schultz 2005; Chatelet et al. 2011; Gerzon et al. 2015;
72 Hochberg et al. 2015; Santarosa et al. 2016; Shtein et al. 2016), and to be
73 affected by environmental parameters (Schubert et al. 1999). Only a few studies
74 analyzing anatomical features of xylem in mature *Vitis* trunks have been
75 published (Zimmermann and Jeje 1981; Ewers et al. 1990; Tibbetts and Ewers
76 2000; Shtein et al. 2016).

77 Another interesting feature of *Vitis* xylem is the bimodal distribution pattern of
78 vessel diameters, meaning two distinct vessel size groups – wide and narrow
79 (Carlquist 1985; Ewers et al. 1990; Wheeler and LaPasha 1994; Shtein et al.
80 2016). Wide diameter vessels are considered to be more hydraulically efficient,
81 and tend to be more vulnerable to embolism within the same species (Sperry and
82 Tyree, 1988; Lo Gullo and Salleo, 1991; Hargrave et al., 1994; Cai and Tyree,
83 2010; Christman et al., 2012; Scoffoni et al., 2016). The accepted "air-seeding"
84 theory suggests that the increased vulnerability to embolism of wide vessels is
85 linked to their enlarged total area of intervessel pits. A wide pit area raises the
86 average size of the "rare" largest pore, consequently increasing the risk of air
87 seeding (Choat et al. 2003; Wheeler et al. 2005; Jansen et al. 2009; Cai and
88 Tyree 2010).

89 Most cultivated vineyards worldwide are located in semi-arid and arid regions
90 where drought stress is prevalent (Chaves et al. 2007). Nevertheless, compared to
91 other woody plants, grapevines are often described as relatively vulnerable to
92 drought stress (Choat et al. 2010; Zufferey et al. 2011; Jacobsen and Pratt 2012;
93 Hacke 2015). It has been reported that drought stress induces embolism and a
94 loss of hydraulic function (Schultz and Matthews 1988; Hargrave et al. 1994;
95 Lovisolo et al. 1998; Choat et al. 2010; Brodersen et al. 2014). Drought stress
96 also negatively affects vegetative growth and pruning weight of vines (Matthews

1987; Intrigliolo and Castel 2010; Shellie and Bowen 2014; Munitz et al. 2016).
There is a lack of available information on the effects of drought stress on
hydraulic conductivity resulting from modifications to *Vitis* xylem anatomy, as
only a few studies have examined this subject (Lovisolo et al. 1998; Hochberg et
al. 2015). The current study focuses on the long-term anatomical acclimation to
drought stress of mature *Vitis vinifera* Merlot vines.

103

104 **Materials and Methods**

105 *Plant material and experimental design*

106 This study was carried out in a 100-ha commercial vineyard located in the
107 Judean Plain, Israel (31⁰49'N, 34⁰53'E, elevation 124 m). This region has a semi-
108 arid climate with predominantly winter rainfall (average 463 mm year⁻¹) and high
109 evapotranspiration (average 1512 mm year⁻¹). The vineyard was planted in 1998
110 with *Vitis vinifera* L cv. 'Merlot' grafted to 140 Ruggeri, and trained onto a two-
111 wire vertical trellis. Row direction was North/South with a slight tendency to the
112 West, and vine and row spacing were 1.5 m and 3 m respectively (2222 vines ha⁻¹).
113 The soil was loam (48% sand, 29% silt and 23% clay, field capacity 28 %
114 vol., wilting point 14 % vol.). Pest management and fertilization in the vineyard
115 were applied according to standard local agricultural practice.

116 The experimental design was a complete randomized block design with five
117 irrigation treatments each replicated four times. Each block comprised three rows
118 (one data and two border rows). Each plot comprised 16 vines per line, with the
119 outer two vines at each end being buffer vines and the inner 12 vines being
120 measurement vines (a total of 240 measurement vines, i.e. 12 vines × 5
121 treatments × 4 replicates).

122 *Irrigation treatments*

123 During 2009-2012, five irrigation treatments representing different levels of
124 deficit irrigation were applied as percentages of crop evapotranspiration (ET_c).
125 Crop evapotranspiration was calculated by multiplying reference
126 evapotranspiration (ET_o) by the crop coefficient (K_c), i.e. ET_c = ET_o × K_c. ET_o
127 was calculated using data obtained from the adjacent meteorological station, and
128 K_c was calculated according to Netzer *et al* (2009) following nondestructive
129 measurements of leaf area index. For more details about the irrigation method
130 see Munitz and Netzer (2016). Irrigation treatments followed two different

131 strategies: static irrigation and dynamic (seasonally changing) irrigation.
132 Dynamic treatments involved alternation of the percentage of ET_c along the
133 growing season according to phenological stages (stage I, stage II, stage III) as
134 defined by Kennedy (2002): stage I – from bloom to bunch closure, stage II –
135 from bunch closure to veraison (color change to red) and stage III – from
136 veraison to harvest. Dynamic irrigation treatments were: early deficit (0, 20, 50%
137 of ET_c) and late deficit (50, 20, 20% of ET_c). Static irrigation treatments were:
138 low irrigation (20% of ET_c), medium irrigation (35% of ET_c) and high irrigation
139 (50% of ET_c).

140 *Stem water potential (Ψ_s)*

141 Stem water potential (Ψ_s) was measured using a pressure chamber (Arimad 2,
142 Kfar Charuv, Israel). Three sunlit, mature, fully-expanded leaves from each plot
143 (12 leaves per treatment) were bagged 2 h prior to measurement in plastic bags
144 covered with aluminum foil. The time elapsing between leaf excision and
145 chamber pressurization was less than 15 s. The measurements were conducted
146 one day before irrigation was applied.

147 *Trunk diameter*

148 Measurements were performed monthly with a digital caliper (075430, Signet,
149 Taiwan) on 48 vines per treatment (12 vines per plot \times 4 replicates). In order to
150 obtain consistent data, all measured vines (240) were marked 30 cm above
151 ground with colored tape, and all measurements were taken at this point.

152 *Anatomical sampling*

153 At the end of the experiment (December 2012) xylem cores from representative
154 vines were sampled 50 cm above ground with an increment borer (5.15 mm Core
155 3-Thread 8", Haglof, Sweden). Twelve cores were sampled from each treatment
156 (3 cores per plot \times 4 replicates, 60 cores total). Trunk diameter (D ; mm) at the
157 drilling location was recorded. Cores were placed in sterilized water and stored at
158 4°C until cross sectioned with a sliding microtome (NR17800, Reichert, Austria)
159 at a thickness of 90 μ m. In order to increase visual contrast, cross sections were
160 stained for 60 s in Reactif Genevois solution (FAHN 1954), then flushed with
161 distilled water. Photographs of stained cross sections were obtained using a
162 stereo microscope (Olympus SZ2-ILST) coupled with a digital camera (Olympus
163 LC20) equipped with image acquisition software (LCmicro 5.1, Olympus,
164 Tokyo, Japan) at $\times 20$ magnification.

165 *Image analysis*

166 Analysis of cross sections was performed by separately quantifying various
167 parameters in the visible field for each of four recent growth rings (2009-2012)
168 using ImageJ software (Rasband, W.S., ImageJ, U.S. National Institutes of
169 Health, Bethesda, Maryland, USA, <http://imagej.nih.gov/ij/>, 1997-2016). The
170 abbreviations for structural parameters were taken from Scholz *et al.* (2013). The
171 following anatomical parameters were measured (Fig. 1): annual ring width (W_r ;
172 μm), bark width (W_b ; μm), xylem radius (r_x ; μm) and inner xylem radius (r_i ;
173 μm). Vessel lumen area (A_v ; μm^2) and number of vessels (n) were measured using
174 the 'analyze particles' tool (see Fig. 2 for explanation); analyzed area (A ; mm^2)
175 was also measured. A total of 12,177 vessels were measured and used for
176 subsequent hydraulic conductivity calculations. The detailed calculations for
177 trunk and vessel parameters are presented in Table 1.

178 *Theoretical specific hydraulic conductivity (K_s) calculations*

179 The theoretical specific hydraulic conductivity (K_s ; $\text{kg m}^{-1} \text{MPa}^{-1} \text{s}^{-1}$) was
180 calculated using the modified Hagen–Poisuille's equation (Tyree and Ewers
181 1991):

$$K_s = (\pi\rho/128\eta A_w) \sum_{i=1}^n (d_i^4)$$

182 where K_s is the specific hydraulic conductivity, ρ is the density of the fluid in kg
183 m^{-3} (assumed to be 1000 kg m^{-3}), η is the dynamic viscosity of the fluid in MPa s^{-1}
184 (assumed to be $1 \times 10^{-9} \text{ MPa s}^{-1}$), A_w is the area (m^2) of the xylem cross section
185 analyzed, d is the diameter (m) of the i^{th} vessel and n is the total number of
186 vessels in the measured area.

187 Hydraulic conductivity per annual ring (K_{ar} , $\text{kg m}^{-1} \text{MPa}^{-1} \text{s}^{-1}$) was calculated by
188 multiplying the theoretical xylem specific hydraulic conductivity (K_s) by annual
189 growth ring area (A_r , m^2).

190 Frequency classes for calculation of total vessel number and total conductivity
191 were established at intervals of $20 \mu\text{m}$ (Fig. 3). For calculation of vessel density
192 and vessel average diameter, vessels were separated into two size categories
193 ($>100 \mu\text{m}$, $\leq 100 \mu\text{m}$), since *Vitis* has a bimodal distribution of xylem vessels
194 (Fig. 3A).

195 *Statistical analysis*

196 The software program JMP7 (SAS Institute, Cary, NC) was used for all
197 statistical procedures. Data were analyzed via analysis of variance (ANOVA),
198 and means were separated according to the least significant difference (LSD) at p
199 ≤ 0.05 using the Tukey-Kramer test.

200

201 **Results**

202 *Stem vessel distribution*

203 The distribution of stem xylem vessels in all irrigation treatments showed a
204 classic bi-modal pattern. The small vessels ($< 100 \mu\text{m}$) constituted the majority
205 (61.3%) of total vessel number, while the large vessels comprised only 38.7% of
206 total vessels (Fig. 3A). In contrast, the theoretical hydraulic conductivity showed
207 a reverse distribution, where the large vessels contributed 97.2% of total
208 conductivity (Fig. 3B), whereas the contribution of the more abundant small
209 vessels was negligible.

210 *Seasonal changes in trunk diameter*

211 As an integrative indicator of vegetative growth, seasonal changes in trunk
212 diameter were monitored monthly during 2011-2012 (following two years of
213 differential irrigation application after 11 years of identical irrigation). Seasonal
214 trends of trunk diameter development were similar in both years in all irrigation
215 treatments (Fig. 4); an increase in trunk diameter began two weeks after bud
216 break and continued until stage II (mid-June), then remained stable until the next
217 season. In 2011, a decrease in trunk diameter was apparent during stage III, in all
218 irrigation treatments. Vines in different irrigation treatments showed significant
219 differences in trunk diameter throughout the entire experimental period (Fig. 4).
220 Among static irrigation vines, trunk diameter was positively correlated with
221 applied water amounts, even though the trunk of the medium irrigation vines was
222 slightly narrower than expected (Fig. 4A). In the dynamic irrigation treatments,
223 the early deficit vines exhibited the narrowest trunk diameter of all vines in all
224 irrigation treatments during the entire measuring period. The late deficit vines
225 had an intermediate trunk diameter throughout the measuring period (Fig. 4B).

226 *Structural parameters*

227 Vines subjected to the static irrigation treatments differed significantly in their
228 annual ring width, with a positive effect of applied water amounts on ring width
229 (Table 2). Within the dynamic irrigation treatments, the late deficit vines had the

230 widest annual ring width (901.5 μm), very similar to the width of the high
231 irrigation vines (Table 2). Surprisingly, the early deficit vines had the narrowest
232 annual ring width (686 μm) even compared to the low irrigation vines (719 μm).
233 The general trend of annual ring area resembled the trend of annual ring width.
234 Ring area was positively affected by increasing water amounts in static treatment
235 vines. In dynamic irrigation treatments, early deficit vines had the smallest
236 annual ring area of the five treatments, while the late deficit vines had a
237 relatively large ring area, intermediate between that of the high and medium
238 irrigation vines (Table 2).

239 The density of 'small' ($\leq 100\mu\text{m}$) and 'large' ($>100\mu\text{m}$) vessels was not
240 significantly affected by irrigation treatments, although a reduction in the density
241 of 'small' vessels in high irrigation vines was observed. The 'large' ($>100\mu\text{m}$)
242 vessel diameter of the high irrigation vines was significantly wider than that of
243 the low and medium irrigation vines. In the dynamic irrigation treatments, early
244 deficit vines had significantly narrower 'large' vessels than all vines in all other
245 irrigation treatments, while the late deficit vines had the widest (Table 1). The
246 trend for 'small' ($\leq 100\mu\text{m}$) vessel diameter was less clear, with early deficit and
247 medium irrigation vines exhibiting significantly wider vessels than all other
248 vines. The trend in specific hydraulic conductivity was similar to that of 'large'
249 ($>100\mu\text{m}$) vessel diameter, where the high irrigation and late deficit vines had
250 significantly higher hydraulic conductivity (Table 1) than vines in other
251 treatments. Hydraulic conductivity per annual ring increased significantly with
252 increasing water amounts in the static irrigation treatments, whereas in dynamic
253 treatments the early deficit vines had the lowest conductivity, while the late
254 deficit vines had high conductivity (slightly lower than the high irrigation vines).

255 The relationship between hydraulic conductivity per annual ring and seasonal
256 water amount (Fig. 6a) was weak and non-significant ($R^2 = 0.21$), while the
257 relationship between hydraulic conductivity per annual ring and water amounts
258 applied during stage I (bloom to bunch closure, Fig. 5b) was stronger and
259 significant ($R^2 = 0.60$, $p < 0.001$).

260 *Stem hydraulic conductivity distribution among vessel size classes*

261 Specific stem hydraulic conductivity was calculated separately for each vessel
262 size class (Fig 6). Among static irrigation treatments, the conductivity
263 distribution was similar, but several differences among treatments were

264 observed. In low irrigation vines a higher percentage of the calculated hydraulic
265 conductivity was derived from narrow vessel classes, in the medium irrigation
266 vines - from wide vessel classes, and in the high irrigation vines - from the
267 widest vessel classes (Fig 6a). In the dynamic irrigation treatments, the early
268 deficit vines had a higher amount of hydraulic conductivity derived from
269 narrower frequency classes, while the hydraulic conductivity in late deficit vines
270 shifted towards the wide frequency classes (Fig 6b).

271 *Stem water potential*

272 Significant differences in water potential (Ψ_s) between vines in different
273 irrigation treatments were observed during stages II and III (Fig. 7). The daily
274 trend of Ψ_s was similar among treatments, with a steep decrease in Ψ_s values
275 being recorded throughout the morning, followed by stabilization and
276 improvement in Ψ_s during the afternoon (Fig. 7). In stage II an improvement in
277 Ψ_s values during the afternoon was apparent only in the high and medium
278 irrigation vines (Fig. 7B). On both measuring days, the high irrigation vines had
279 the highest Ψ_s values during the course of the day, the medium irrigation vines
280 were at an intermediate level and the low irrigation vines had the lowest Ψ_s . In
281 the dynamic irrigation treatments, the early deficit vines had low Ψ_s values
282 during stage II (lower than the low irrigation vines) and intermediate values
283 during stage III (resembling those of the medium irrigation vines). The late
284 deficit vines had low Ψ_s values on both dates, even compared to the values of the
285 low irrigation vines (Fig. 7).

286

287 **Discussion**

288 *Vegetative growth*

289 Vegetative growth can serve as a good indicator of water availability (Tyree and
290 Ewers 1991; Munitz et al. 2016). In the present study we continuously monitored
291 trunk growth. In all irrigation treatments, an increase in trunk diameter occurred
292 mainly early in the season (from two weeks before blooming until bunch closure)
293 (Fig. 4). Early season trunk growth has been previously reported in Merlot (Ton
294 and Kopyt 2004) and in other *Vitis vinifera* cultivars (Myburgh 1996; Ton and
295 Kopyt 2004; Intrigliolo and Castel 2007; Montoro et al. 2011; Papi and Storchi
296 2012; Edwards and Clingeleffer 2013).

297 The high irrigation and late deficit vines, which received higher water amounts
298 early in the season, exhibited the widest trunk diameter of all vines. Similarly,
299 annual ring width and area, which represent annual vegetative growth, were also
300 positively correlated with high irrigation early in the season (Stage I). The high
301 irrigation and late deficit vines had significantly wider ring width and area in
302 comparison to the low irrigation and early deficit vines (Table 2). The dominance
303 of early season vegetative growth in *Vitis vinifera* can be explained by the fact
304 that cambial activity to produce new vascular elements takes place mainly during
305 the early stage of the growing season (until 20 days after bunch closure,
306 Bernstein and Fahn, 1960).

307 *Hydraulic structure*

308 A significant increase (9 - 11%) in the large vessel diameter was recorded in the
309 high irrigation and late deficit vines (Table 2), even though no significant
310 difference in the density of the large vessels was found. This implies that water
311 availability early in the season affects large vessel diameter rather than vessel
312 density. The same effect of drought stress reducing average vessel diameter has
313 been reported in *Vitis vinifera* shoots (Lovisolo et al. 1998) and petioles
314 (Hochberg et al. 2015). Interestingly, in small vessels the opposite was found,
315 where the vessels of the early deficit vines, which received minimal water early
316 in the season, exhibited the widest diameter (Table 2). Although the small
317 vessels comprised the majority of the total vessels (61%), they contributed only a
318 negligible 3% of total hydraulic conductivity (Fig. 3). A similar phenomenon of
319 dominance of wide diameter vessels with respect to total hydraulic conductivity
320 has also been recorded in other species (Hargrave et al. 1994; Tibbetts and Ewers
321 2000).

322 From inspection of the hydraulic conductivity distribution, it can be deduced that
323 high water amounts early in the season result in a higher percentage of hydraulic
324 conductivity derived from wider frequency classes (Fig. 6). This phenomenon is
325 more pronounced in late deficit vines, possibly due to their dynamic irrigation
326 treatment. It is well known that in *Vitis*, as in many other lianas, wide vessels are
327 formed at the beginning of the growing period and narrow vessels are formed at
328 the end (extreme diffuse-porous), causing a bi-modal distribution of vessels
329 (Pratt 1974; Kozlowski 1983; Ewers et al. 1990; Wheeler and LaPasha 1994).
330 Applying high irrigation amounts during the formation of wide vessels and

331 reducing water allocation during the formation of narrow vessels (late deficit),
332 should result in larger wide vessels and smaller narrow vessels. This will lead to
333 an increased proportion of hydraulic conductivity being derived from wide
334 vessels. As a result, late deficit vines are expected to be more susceptible to
335 embolism formation in comparison to low irrigation vines.

336 Specific hydraulic conductivity (K_s) represents the conducting efficiency of the
337 xylem tissue (Tyree and Ewers 1991). The high irrigation and late deficit vines
338 had significantly increased K_s (24 - 33%) compared to other vines (Table 2). This
339 means that limited water availability early in the growth season (bloom to bunch
340 closure) results in decreased K_s . Since there is a good correlation between
341 measured and calculated hydraulic conductivity (Salleo et al. 1985; Hargrave et
342 al. 1994; Lovisolo et al. 1998; Nolf et al. 2017) our theoretical K_s results may
343 indicate an actual change in the hydraulic conductivity of vines in response to
344 drought stress.

345 Hydraulic conductivity per annual growth ring (K_{ar}) is an integrated parameter
346 combining both hydraulic conductivity (K_s) and vegetative growth (trunk
347 diameter and ring width). As with ring area and hydraulic conductivity, the high
348 irrigation and late deficit vines had significantly increased hydraulic conductivity
349 per annual ring (K_{ar} , Table 2). Interestingly, the high irrigation vines had 9%
350 higher K_{ar} (not significant) than the late deficit vines. This difference can be
351 attributed to the reduction of water amounts in late deficit vines during bunch
352 closure, while cambial activity in the stem persisted for a further 20 days
353 (Bernstein and Fahn 1960).

354 Reinforcement of the notion that most of the vegetative growth and xylem
355 development occur early in the season can be found in the correlation between
356 the amounts of applied water and hydraulic conductivity per annual ring, K_{ar}
357 (Fig. 5). While annual water applied had a weak and non-significant correlation
358 with K_{ar} ($R^2 = 0.21$), water amount applied during stage I was strongly and
359 significantly correlated to K_{ar} ($R^2 = 0.6$, $P < 0.001$).

360 *Water potential*

361 Stem water potential is known to be a sensitive indicator of vine water status
362 (Choné et al. 2001; Munitz et al. 2016). Indeed, on both measuring days static
363 irrigation vines differed significantly in their stem water potentials, according to
364 the water amounts applied, throughout the entire day. Those differences in stem

365 water potential were present from bunch closure until harvest (Munitz et al.
366 2016). Interestingly, late deficit vines were more drought stressed (more negative
367 stem water potential) than low irrigation vines on both measuring days, even
368 though they received on average 31% more water prior to the measuring days.
369 Those differences in stem water potential cannot be attributed to a broader
370 canopy, since the late deficit and low irrigation vines had similar leaf area on
371 measuring days (Munitz et al. 2016). Water potentials of -1.4 MPa, recorded on
372 both measuring days, have been reported to cause a 30 - 80 % decrease in
373 hydraulic conductivity of *Vitis vinifera* shoots (Alsina et al. 2007; Choat et al.
374 2010; Jacobsen and Pratt 2012).

375 The increased drought stress in late deficit vines can be explained by a greater
376 hydraulic conductivity loss. As stated before, wide vessels are more susceptible
377 to embolism formation. Late deficit vines, with a higher percentage contribution
378 of wide vessels to total hydraulic conductivity, are expected to experience greater
379 hydraulic loss at a similar water potential. Increased hydraulic loss will, in turn,
380 lead to increased drought stress e.g. more negative water potential (Tyree et al.
381 1991). Another explanation for the increased drought susceptibility of late deficit
382 vines compared with low irrigation vines, can be found by examining their
383 Carlquist's "vulnerability index" (1977). The index is calculated by dividing
384 average vessel diameter by vessel density, where a lower value is interpreted as
385 greater redundancy of vessels and improved capability of withstanding drought
386 stress. The large vessels of the late deficit vines have an index of 17.0 while low
387 irrigation vines have an index of 14.9.

388 *Structural parameters as compared to values from literature*

389 Generally, our results seem to be in agreement with values presented in the
390 literature. The annual increase in trunk diameter of mature vines measured in this
391 study (1.5 – 2.5 mm, Fig. 4), is similar to that reported for a number of *Vitis*
392 *vinifera* cultivars (0.5 - 3.5 mm) (Bernstein and Fahn 1960; Myburgh 1996; Ton
393 and Kopyt 2004). Similarly, the range of annual ring width measured in this
394 study (720 - 901 μm) is consistent with values reported for mature *Vitis vinifera*
395 cultivars (100 - 1300 μm) (Perold 1927; Bernstein and Fahn 1960), and the range
396 of annual ring area found in this study (104 - 134 mm^2) resembles that of
397 Cabernet Sauvignon vines (120 - 240 mm^2 , Shtein *et al.*, 2016).

398 The average diameter of large vessels measured in this study (147 - 158 μm) is
399 considerably smaller than that reported for *Vitis vinifera* cv. Cabernet Sauvignon.
400 While in the current study water availability of Merlot vines in different
401 irrigation regimes triggered a maximal difference of 11 μm in vessel diameter
402 (Table 2), the difference between the two cultivars stands at more than 50 μm .
403 This implies an inherent genetic distinction in stem xylem anatomy between *Vitis*
404 *vinifera* cultivars, as reported previously for petioles and shoots (Chouzouri and
405 Schultz 2005; Chatelet et al. 2011; Tombesi et al. 2014; Gerzon et al. 2015;
406 Hochberg et al. 2015; Santarosa et al. 2016). Typical values of specific hydraulic
407 conductivity of liana stems (Milburn 1979) are 65 - 349 $\text{kg m}^{-1} \text{MPa}^{-1} \text{s}^{-1}$; our K_s
408 results (142 - 188 $\text{kg m}^{-1} \text{MPa}^{-1} \text{s}^{-1}$) are in the middle of this range. Values of K_{ar}
409 reported for *Vitis vinifera* cv. Cabernet Sauvignon (0.07 - 0.11, $\text{kg m}^{-1} \text{MPa}^{-1} \text{s}^{-1}$)
410 are considerably higher than those calculated in this study, due to the wider
411 vessels and ring area measured in Cabernet Sauvignon vines.

412 *Conclusions*

413 In the current study, we conducted a comprehensive structural analysis of the
414 mature stem xylem of *Vitis vinifera*, combined with physiological measurements.
415 The stem comprises the perennial part of the deciduous vine and its anatomical
416 structure constitutes the long term "memory" of the vine, yet very little
417 information about the anatomical features of mature *Vitis* stems is available. One
418 example of this "memory" is the fact that the current year's vine canopy develops
419 while consuming water conducted through vessels differentiated in previous
420 years. Most of the vine's canopy develops in the early stages of the growing
421 season, about 60 days from budbreak (Ben-Asher et al. 2006; Intrigliolo et al.
422 2008; Romero et al. 2010; Munitz et al. 2016). Cambial tissue begins its activity
423 about two weeks after budbreak (Bernstein and Fahn 1960). Vessels become
424 hydraulically active about four weeks after their initial differentiation is initiated
425 (Halis et al. 2012; Hacke 2015): two weeks for differentiation, expansion and
426 formation of secondary walls and at least two additional weeks for the creation of
427 perforation plates by autolysis of axial cell walls. Practically this means that
428 current year vessels are functional no less than 54 days after budbreak, when
429 canopy development has almost ceased.
430 There is a lack of information about the effects of drought stress on *Vitis* xylem
431 structure (Lovisololo et al. 1998), especially in mature stems. Our research can

432 contribute to the understanding of mature stem xylem structure and how it is
433 affected by drought stress in the long term.

434 *Acknowledgments*

435 This study was partly sponsored by the Israeli Wine Grape Council. The authors
436 thank Michal Akerman and Dan Aluf for their assistance in setting up this study,
437 and the dedicated growers of Kibbutz Hulda: Silvio Feldman, Robbie Handel and
438 Yigal Gad. We particularly thank Yechezkel Harroch and Elazar Quinn for
439 assisting in the field and to Ami Charitan and Ziv Charit from Netafim for
440 donating the irrigation system. We thank the agronomists of Barkan Winery,
441 Elad Gutman and Yakov Cohen-Achdut for their collaboration. We also thank
442 Eran Harkabi from the Israel Ministry of Agriculture and Rural Development for
443 his assistance.

References

Table 1. Calculations used for trunk and vessel parameters.

Parameter	Abbreviation	Unit	Formula
Vessel diameter	d	μm	$d = (4 * A_v / \pi)^{0.5}$
Vessel density	V_D	mm^{-2}	$V_D = n/A$
Trunk radius	R	μm	$R = D/2$
Xylem radius	r_x	μm	$r_x = R - W_b$
Annual ring area	A_r	mm^2	$A_r = \pi * (r_x)^2 - \pi * (r_i)^2$

Table 2. Water amounts, anatomic and hydraulic parameters. ‘Hulda’ Merlot vineyard, 2009 - 2012.

Irrigation treatment	Water amount (mm season ⁻¹)	Annual ring width (μm)	Annual ring area (mm ²)	Large vessel density (mm ⁻²)	Small vessel density (mm ⁻²)	Large vessel average diameter (μm)	Small vessel average diameter (μm)	Specific hydraulic conductivity (kg m ⁻¹ MPa ⁻¹ s ⁻¹)	Hydraulic conductivity per annual ring (kg m MPa ⁻¹ s ⁻¹)
Low	105	719.9 ^{bc}	104.4 ^{bc}	9.9	16.9	147.9 ^b	37.5 ^b	142.5 ^b	0.0152 ^b
Medium	184	835.6 ^{ab}	124.2 ^{ab}	9.6	14.7	147.1 ^b	43.3 ^a	144.0 ^b	0.0179 ^b
High	256	891.4 ^a	141.5 ^a	10.3	12.6	154.9 ^a	40.3 ^b	188.6 ^a	0.0273 ^a
Early deficit	143	686.0 ^c	100.9 ^c	9.7	15.5	142.1 ^c	45.5 ^a	127.2 ^b	0.0128 ^b
Late deficit	141	901.5 ^a	134.3 ^a	9.3	15.8	158.5 ^a	38.3 ^b	188.3 ^a	0.0257 ^a

Values represent means (n = 12). Within each column, means followed by different letters are significantly different ($P < 0.05$) according to Tukey's test.

Figure legends

Figure 1. Schematic cross section diagram with abbreviations used for trunk parameter calculations.

Figure 2. Stem cross section of *Vitis vinifera* cv. Merlot. (A) Cross section image as acquired by stereo microscope. (B) Image processing to 8-bit. (C) Image conversion to black and white (binarization) and selection of annual ring to be analyzed (yellow line). (D) Measurement of vessel area.

Figure 3. (A) Distribution of stem xylem vessels according to diameter classes (μm) in Merlot vines of all irrigation treatments. (B) Distribution of hydraulic conductivity according to diameter classes (μm) in Merlot vines of all irrigation treatments. Vessel classes were divided into two size categories: $\leq 100 \mu\text{m}$ (black bars) and $> 100 \mu\text{m}$ (gray bars). Data represent vessels from all irrigation treatments during 2009-2012, $n = 12177$ vessels.

Figure 4. (A) Biennial pattern of trunk diameter development of Merlot vines exposed to low irrigation (closed circles), medium irrigation (closed squares) and high irrigation (closed triangles), in 2011 and 2012. (B) Biennial pattern of trunk diameter development of Merlot vines exposed to early deficit (open circles) and late deficit (open squares), in 2011 and 2012. Each point is the mean of 48 vines (12 vines per replicate). The vertical bars denote one standard error.

Figure 5. (A) Relationship between annual water applied and hydraulic conductivity per annual growth ring in Merlot vines of all irrigation treatments. (B) Relationship between water amount applied during stage I (bloom to bunch closure) and hydraulic conductivity per annual growth ring in Merlot vines of all irrigation treatments. Each point is the mean of 12 vines (3 vines per replicate). The vertical bars denote one standard error.

*Significant at $P < 0.001$.

Figure 6. (A) Distribution of hydraulic conductivity according to diameter classes (μm) in Merlot vines exposed to low irrigation (solid line), medium irrigation (dotted line) and high irrigation (dashed line). (B) Distribution of hydraulic conductivity according to diameter classes (μm) in Merlot vines exposed to early deficit (solid line) and late deficit (dashed line). Data represent vessels from all analyzed years (2009-2012), $n = 12177$ vessels.

Figure 7. (A) Daily pattern of stem water potential of Merlot vines exposed to low irrigation (closed circles), medium irrigation (closed squares), high irrigation (closed triangles), early deficit (open circles) and late deficit (open squares), on 10/08/11. (B) Daily pattern of stem water potential of Merlot vines exposed to low irrigation (closed circles), medium irrigation (closed squares), high irrigation (closed triangles), early deficit (open circles) and late deficit (open squares), on 26/07/12. Each point is the mean of 12 leaves (3 vines per replicate). The bars denote one standard error.

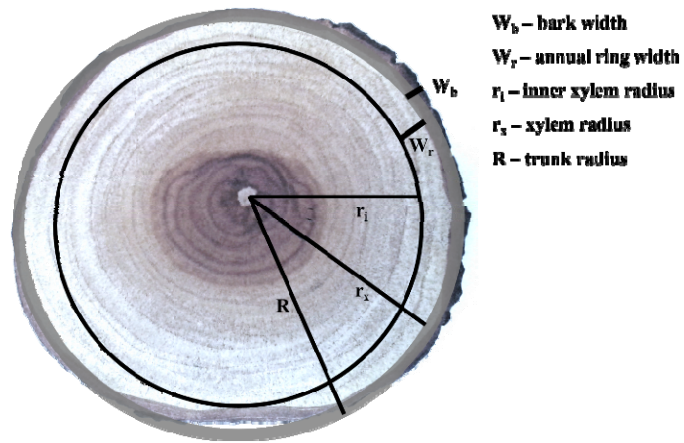


Fig.

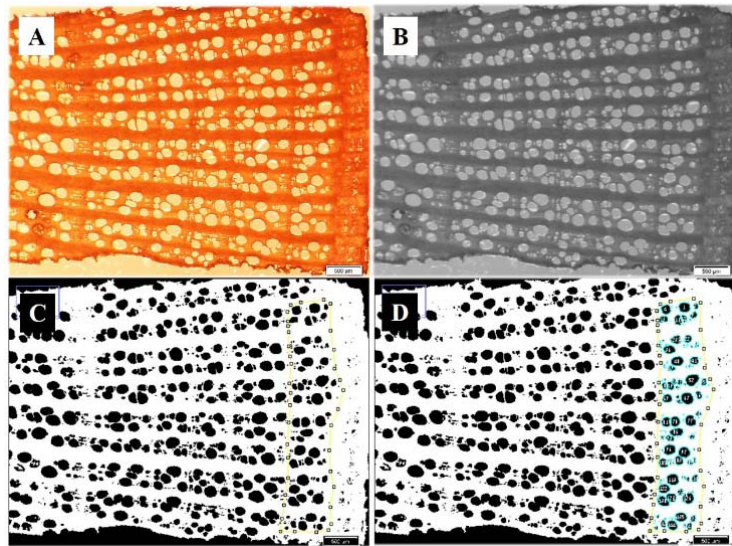


Fig. 2

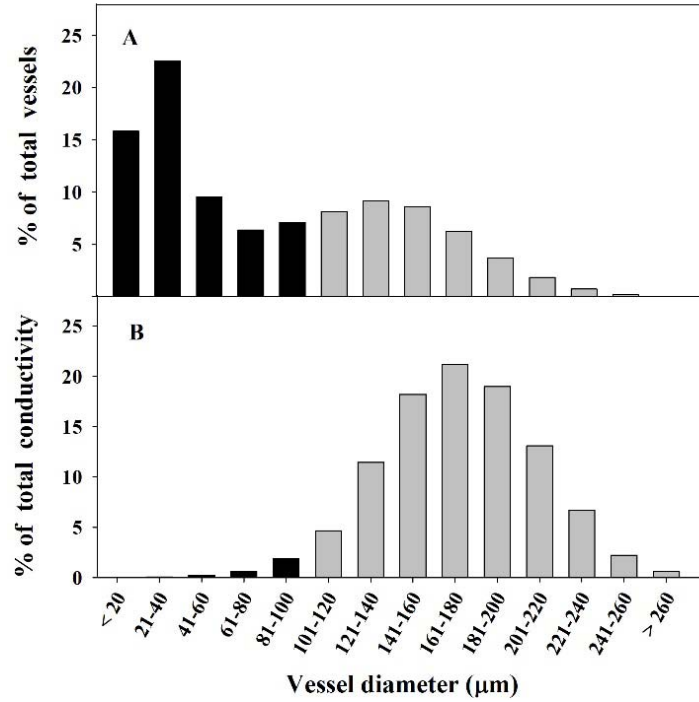


Fig. 3

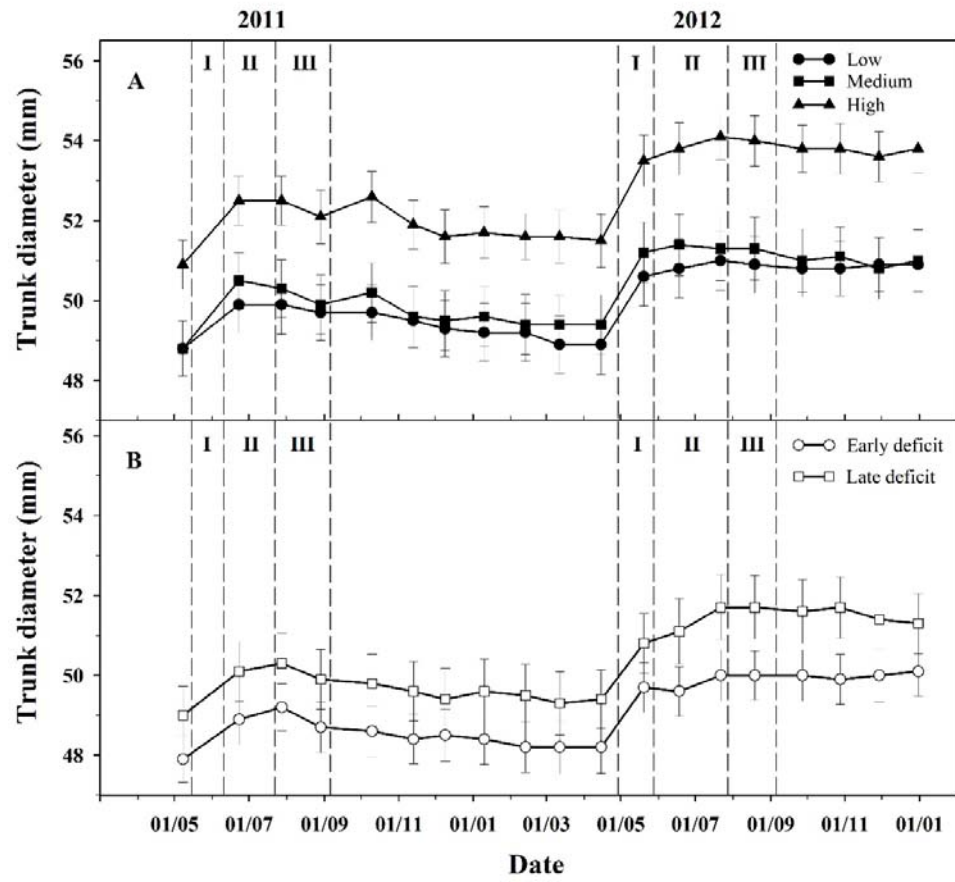


Fig. 4

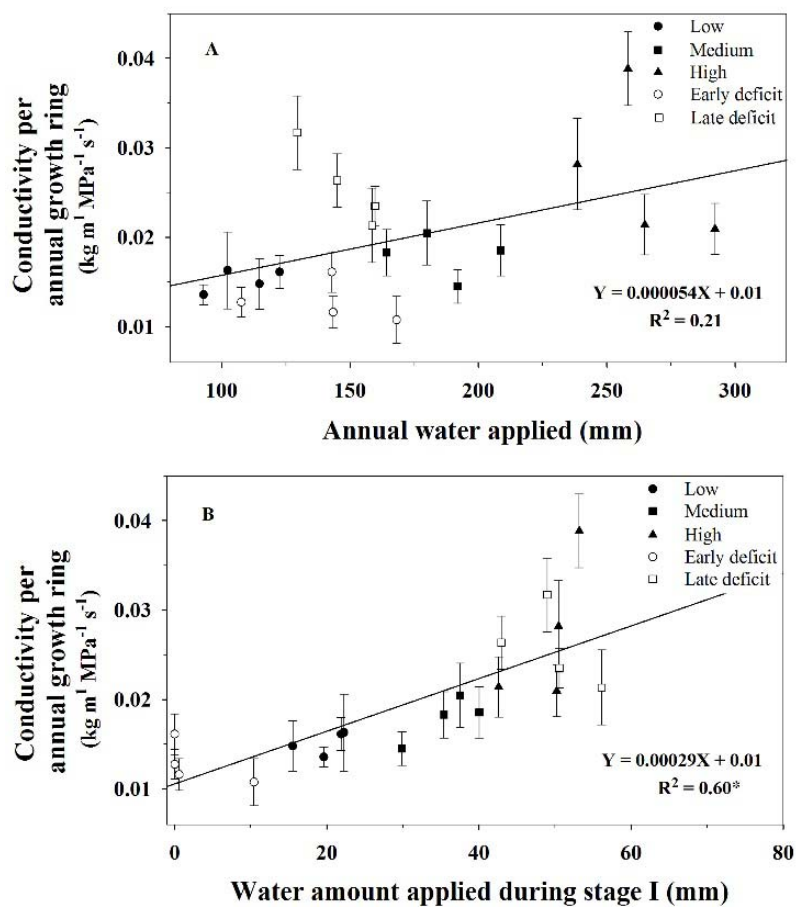


Fig. 5

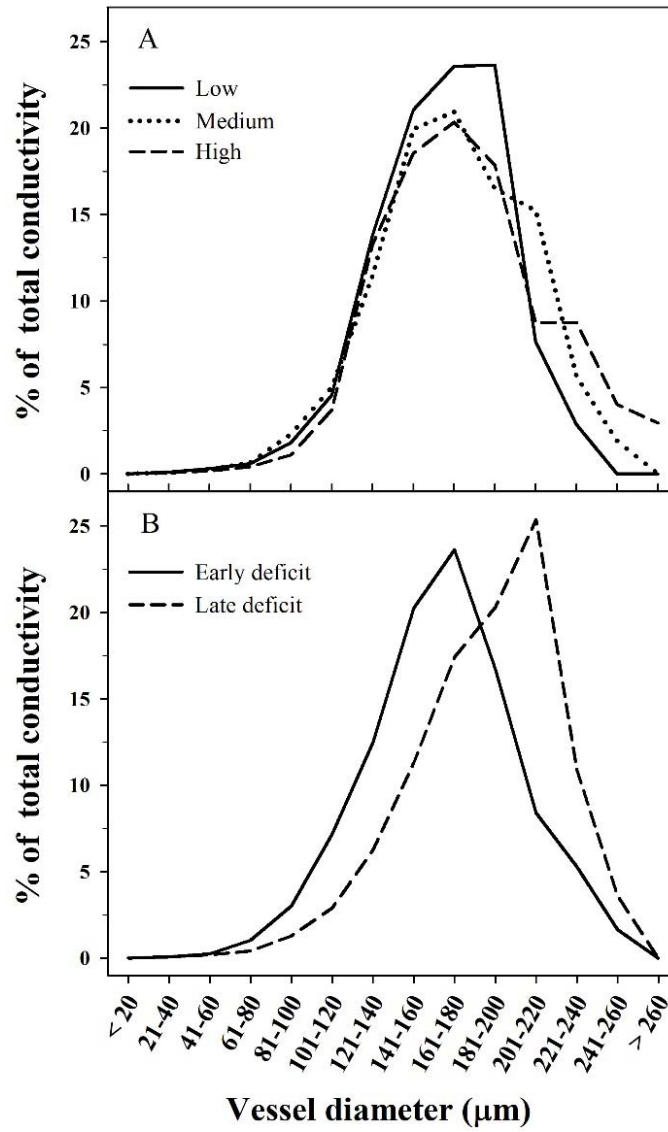


Fig. 6

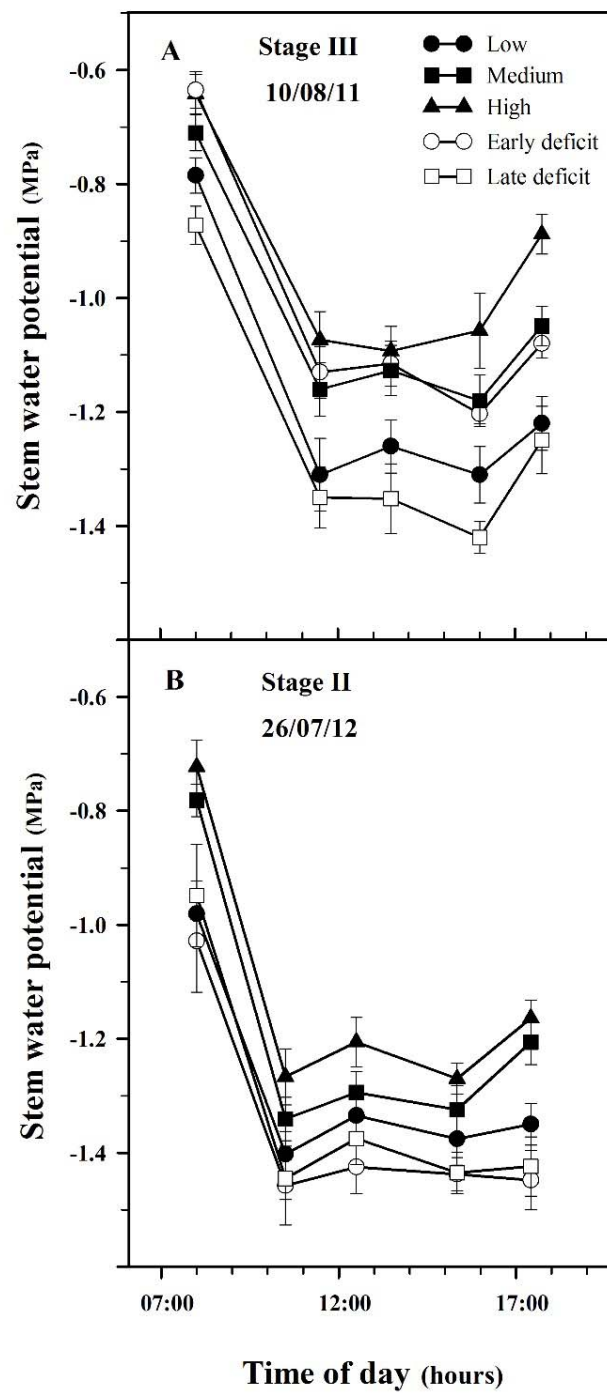


Fig. 7